

# XFlow: An algorithm for extracting ion chromatograms

Mathew Gutierrez<sup>1</sup>, Rob Smith<sup>1\*</sup>

<sup>1</sup>Department of Computer Science University of Montana Missoula, MT, USA

mathewgutierrez00@gmail.com

[robert.smith@mso.umt.edu](mailto:robert.smith@mso.umt.edu)

Authors contributed equally to this work.

## Abstract

Mass spectrometry is a fundamental tool for modern proteomics. The increasing availability of mass spectrometry data paired with the increasing sensitivity and fidelity of the instruments necessitates new and more potent analytical methods. To that end, we have created and present XFlow, a feature detection algorithm for extracting ion chromatograms from MS1 LC-MS data. XFlow is a parameter-free procedurally agnostic feature detection algorithm that utilizes the latent properties of ion chromatograms to resolve them from the surrounding noise present in MS1 data. XFlow is designed to function on either profile or centroided data across different resolutions and instruments. This broad applicability lends XFlow strong utility as a one-size-fits-all method for MS1 analysis or target acquisition for MS2. XFlow is written in Java and packaged with JS-MS, an open-source mass spectrometry analysis toolkit.

## Introduction

Mass spectrometry is a popular approach for measuring the sample-bound content and quantity of a variety of classes of molecules across a broad range of applications including pharmaceuticals,

27 forensics, biochemistry, and food science. All applications of mass spectrometry have a common  
28 problem: the instrument itself does not provide measurements of molecules nor their identities, but  
29 rather produces raw data that must be rendered human-interpretable through the application of data  
30 processing algorithms.

31

32 According to community perceptions, advancements in software have lagged behind the steady  
33 pace of instrumentation advancements.<sup>1</sup> Unlike other computational science fields (such as  
34 genomics) where several foundational computational problems are regarded as solved, most mass  
35 spectrometry users feel that significant problems in computational mass spectrometry remain  
36 unsolved<sup>1</sup> despite (in some cases) dozens of published algorithms designed to address them.<sup>2</sup>  
37 Beyond user sentiment, the experimental influence of algorithm selection suggests that the analysis  
38 and advancement of computational mass spectrometry algorithms is a valuable pursuit.<sup>3</sup>

39

40 Mass spectrometry systems generate datasets that quantify counts of charged particles at specific  
41 mass-to-charge (m/z) values. In liquid chromatography-mass spectrometry (LC-MS) systems,  
42 these measurements are taken over the time (retention time or RT) required for the molecules to  
43 elute from a chromatography column designed to slow or speed the migration of the molecules  
44 depending on particular physico-chemical properties such as size, or polarity.

45

46 Mapping the raw LC-MS data points to particular classes of molecule (say, a particular peptide at  
47 a particular charge state) provides both an accurate count of the relative abundance of that molecule  
48 class (through integrating the intensities in those points) and discriminatory information about the  
49 identity of the molecule, as the charge state and uncharged mass can be derived through the m/z

50 gap present between isotopic-specific sub-signals (extracted ion chromatograms or XICs) in the  
51 molecule's signal (see Figure 1).

52 **Fig 1. 3d Isotopic Envelope.** In this figure are five extracted ion chromatograms (XIC) bounded  
53 by yellow rectangles. Each XIC is composed of points, each with m/z, RT and intensity (denoted  
54 by color and height on z axis). Each XIC is the evidence of an isotope of a specific molecule.  
55 The group of five XICs is referred to as an isotopic envelope, or feature, seen bounded by the red  
56 rectangle.

57  
58 Some existing algorithms attempt to resolve the features directly from the point data (e.g. OpenMS  
59 FFC<sup>4</sup>). Other algorithms split this process into two steps. First, two step algorithms cluster points  
60 into XICs, sometimes called isotopic traces (or features<sup>5</sup>). Second, by clustering XICs into isotopic  
61 envelopes (sometimes also called features<sup>5</sup>) (see Figure 1). This two stage approach maximizes  
62 the utilization of available information, and serves to reduce the amount of data by allowing a  
63 summary of each XIC to be used to find isotopic envelopes instead of cumbersome point data.

64

65 This manuscript presents *XFlow*, a novel algorithm for extracting ion chromatograms from LC-  
66 MS data. XFlow outperforms existing XIC algorithms evaluated recently on a benchmark human-  
67 curated dataset and provides qualitative evidence in support of high-function on alternative  
68 datasets. The output of XFlow can be used in conjunction with the XIC clustering algorithm XNet<sup>6</sup>  
69 to map raw data points from an LC-MS run into the signal groups corresponding to particular  
70 molecules at particular charge states.

71

72 A recent XIC benchmark study<sup>7</sup> noted that Massifquant<sup>8</sup>, a Kalman filter-based XIC algorithm,  
73 performed well against other popular algorithms on a large set of hand-annotated XICs.  
74 Massifquant uses a Kalman filter to model XICs as time-series events where the probability of  
75 membership of a proximate point in the next scan is a factor of the m/z of previous points in the

76 putative XIC. Massifquant has several drawbacks. It has a very large possible parameter space,  
77 takes considerable time to run, and lacks an objective or automatic approach to optimize  
78 parameters. Still, it outperformed all other evaluated algorithms on a large human-curated dataset.

79

80 Perhaps the principle theoretical advantage of Massifquant is that it attempts to assemble point  
81 membership in XICs as a function of the probability of a given point being a member of a given  
82 proto-XIC.

83

84 XFlow adopts a similar probabilistic approach to constructing XICs. However, it does so with two  
85 notable differences. First, the order of the point assembly runs from most intense to least intense  
86 instead of from last in retention time to first. Second, the probability function is directly calculable,  
87 and does not depend on Kalman filters, which require large matrices that are expensively updated  
88 for every point.

89

90 XFlow is the first algorithm that leverages intensity order to iteratively construct XICs. Other  
91 algorithms use less rich sources of information. Shape filters (for example, matchedFilter<sup>9</sup> and  
92 centWave<sup>10</sup>) tend to degrade at lower intensities and are expensive to optimize for each signal in  
93 a run. Massifquant<sup>8</sup> and MaxQuant<sup>11</sup> both build XICs scan by scan, though in reverse order. Due  
94 to the Gaussian shape of XICs, this guarantees that the least confident information is the most  
95 relied upon in both of these algorithms, ensuring suboptimal performance.

96

97 The core idea of XFlow is the hypothesis that the most intense points in a mass spectrometry run  
98 also have the most accurate m/z measurement. Therefore, intensity of a point can be used as a

99 surrogate for confidence. XFlow leverages this assumption to build XICs starting with the highest  
100 intensity points as seeds for putative XICs.

101

## 102 Methods

103 XFlow casts ion chromatogram extraction as a clustering problem, where points are clustered into  
104 XICs. XFlow creates an initially unlinked graph where each point from an .mzml file (either  
105 centroid or profile) becomes a vertex. XFlow groups points together in order of descending  
106 intensity by creating links between points nearby in space and intensity. The growing clusters are  
107 referred to as “XIC trees”, as each cluster is unique and acyclical in the graph. Due to the  
108 relationship between intensity and confidence, each XIC tree is initiated with the highest  
109 confidence possible.

110

111 Unlike most XIC algorithms, XFlow is designed to be agnostic to instrument and to whether the  
112 data is centroided or profile. Unlike any published XIC algorithm, it is also parameter-free. XFlow  
113 self-calibrates based on three parameters automatically derived from each run: minimum m/z  
114 separation, minimum RT separation, and a two-dimensional grid of the standard deviation of the  
115 intensity across the file. The minimum m/z separation between any two points belonging to the  
116 same scan is a proxy for the resolution of the machine, and the minimum RT separation between  
117 two consecutive scans is a proxy for sampling-rate of the machine. The two-dimensional grid of  
118 standard deviation of intensities is used by XFlow to determine a points candidacy by comparison  
119 with its neighbors, and not across the file as a whole.

120

121 Using the two-dimensional grid of intensity standard deviation, XFlow determines whether each  
122 point ( $p_i$ ) in the set of all points ( $\mathbf{P}$ ) is permitted to enter into consideration and initiate an XIC tree.  
123 The justification for this thresholding is two part. The primary consideration of thresholding is to  
124 limit the admission of noise into the final output, while the secondary consideration is to reduce  
125 the computational burden to only the relevant subset of the data. The study of when and where to  
126 apply intensity thresholding is an ongoing and varied topic of research due to the difficulty of  
127 avoiding bias, limiting noise inclusion, and maximizing signal inclusion.<sup>12</sup> For a  $p_i$  to be  
128 considered, its intensity must be at least one standard deviation above the mean for its  
129 neighborhood for centroid data, and at least three standard deviations above the mean for profile  
130 data. For each  $p_i$  in consideration, a window of comparison within which to compare nearby points  
131 must be constructed. This window of comparison is constructed using the sampling rate and  
132 resolution calculated previously to define an arbitrarily large window such that each  $p_i$  will be  
133 compared with all nearby points that could be in the same XIC. The justification for defining such  
134 a window is purely in the pursuit of limiting the computation required to just the relevant points.  
135 The set of points within this window of comparison will be referred to as  $\mathbf{W}$ . Once the set of points  
136  $\mathbf{W}$  with which to compare to each  $p_i$  has been obtained, the linking process between  $p_i$  and all  
137 points in  $\mathbf{W}$  begins, and each point ( $w_j$ ) in  $\mathbf{W}$  is considered in order of increasing distance from  $p_i$ .  
138 For each  $w_j$  linked to  $p_i$ , the difference between  $p_i$  and  $w_j$  scaled by their distance is subtracted from  
139  $p_i$ 's intensity. In this way, the linking process is driven by  $p_i$ 's intensity, with larger intensity values  
140 resulting in more links. The formula for the effect on  $p_i$ 's intensity for each link can be seen below  
141 in equation 1.

142

143 
$$\text{intensity}(p_{i,t_2}) = \text{intensity}(p_{i,t_1}) - |(\text{intensity}(p_{i,t_2}) - \text{intensity}(w_j)) * \text{distance}(p_i, w_j)| \quad (1)$$

144

145 As links are added between  $p_i$  and points ( $w_j$ ) in  $\mathbf{W}$ , XFlow updates the group id of  $w_j$  to the id of  
146  $p_i$ . This is synonymous with weighted quick union which takes at most  $M \log(N)$  time for  $M$  edges  
147 on  $N$  objects<sup>13</sup>. If it is the case that  $p_i$  and a  $w_j$  belong to the same formative XIC as determined by  
148 a shared canonical point, their candidacy is stripped and the next point ( $w_{j+1}$ ) is brought up for  
149 consideration. In this way XFlow avoids cycles which can cause problems for resolving subgraphs  
150 later. Given that intensity is equivalent to likelihood of participation in an XIC for a point, we can  
151 record confidence in any given link as a function of the difference of  $p_i$ 's intensity before and after  
152 linking the point divided by its intensity before linking (see Eq 2). A high confidence point is one  
153 that is near in space, and similar in intensity.

154

$$155 \quad confidence = \frac{intensity(p_{i,t_1}) - intensity(p_{i,t_2})}{intensity(p_{i,t_1})} \quad (2)$$

156

157 This value is stored such that each link in question has an associated confidence that is a function  
158 of the nearness in both intensity and Euclidean distance (given that the difference is scaled by their  
159 distance) (see Figure 2). The confidence of each link is used for visualization, but as yet does not  
160 affect the composition of the XIC.

161 **Fig 2. XFlow Link Progression.** This figure details the progression of the linking process for a  
162 group of points from inception to near completion. In the figure, you can see the completely  
163 unlinked group of points that form an XIC (1). Next, the highest intensity point in the group is  
164 linked to points with its window of comparison (2). This process continues with the next point,  
165 and then the next in descending order of intensity. (3-6). Until all points above the intensity  
166 threshold have been recovered (7). Note the correlation between confidence and nearness.

167

168

169 Once XFlow has considered all points ( $w_j$ ) in  $\mathbf{W}$  for each  $p_i$ , or exhausted  $p_i$ 's intensity, it begins  
170 the last step, resolving XICs. XFlow resolves XICs by recovering subgraphs created by the points.  
171 The subgraphs are elucidated by iterating over all points and adding any XIC with more than five  
172 points to the database.

173  
174 Algorithmic performance is evaluated on a hand-annotated dataset<sup>14</sup> from a recent study that  
175 presented over 57,000 XICs from a public LC-MS dataset<sup>15</sup> (UPS2). XFlow was compared to the  
176 algorithms centWave<sup>10</sup>, matchedFilter<sup>9</sup>, and MZmine2<sup>16</sup>, selected for comparison as equivalent  
177 open source algorithms. Accurate evaluation with respect to the hand annotated dataset required  
178 point by point comparison. For the chosen algorithms, point data was recovered using the window  
179 output that each provided.

180 For an XIC to be considered appropriately extracted, it must be matched to a corresponding hand  
181 annotated XIC. For the purposes of determining accuracy, we will refer to the set of points  
182 constituting an XIC produced by the software as  $\mathbf{A}$  while the set of points constituting an XIC  
183 produced by hand annotation will be  $\mathbf{H}$ . For an XIC to be considered correctly recovered, the sum  
184 of the intensity of the intersection of points between  $\mathbf{A}$  and  $\mathbf{H}$  must constitute greater than fifty  
185 percent of the sum of the intensity of the points in the hand annotated XIC ( $\mathbf{H}$ ). This fraction of  
186 shared intensity will be referred to as  $S$  (Eq 3).

187  
188

$$S = \frac{\sum \text{intensity}(A \bigcap H)}{\sum \text{intensity}(H)} \quad (3)$$

189

## 190 Results

191  
192 We compared XFlow to several popular publicly available and functionally equivalent algorithms.  
193 XCMS's centWave<sup>10</sup> and matchedFilter<sup>9</sup> algorithms (optimized using Isotopologue Parameter  
194 Optimization<sup>17</sup>) and Mzmine2<sup>16</sup>. Due to the difficulty of obtaining verified XIC datasets,  
195 quantitative validation of algorithmic results for XFlow, centWave, matchedFilter and MzMine2  
196 are limited to the UPS2 dataset, the only dataset with hand annotated XICs. Five other reference  
197 or standard datasets were selected from the PRIDE repository: PXD000790, PXD000792,  
198 PXD003236, PXD008952, PXD011194. These additional files were selected in order to provide  
199 qualitative information. The RAW files were processed using ProteoWizard's msConvert<sup>18</sup>  
200 (Version: 3.0.19277-b582d79cd) to create centroided and profile .mzml files using vendor  
201 centroiding algorithms. Percent recovery of the hand annotated dataset for each algorithm can be  
202 seen in Figure 3.

203

204 **Fig 3. Percent Recovery of Hand Annotated XICs.** Percentage of XICs shared between hand  
205 annotated dataset, and from the set of XICs output by each algorithm recovered from the UPS2  
206 dataset. Note the relatively low accuracy of XIC recovery across all algorithms, XFlow recovering  
207 the most with nearly 40%.

208

209

210 By observing Figure 3, it is apparent that XFlow returns many more XICs from the UPS2 dataset  
211 than do the other algorithms chosen. XFlow also manages to recover results closer to hand  
212 annotation than the other algorithms. The reason for this is likely the specific method of intensity  
213 thresholding XFlow employs, automatically allowing adjustments for each region of the file to be  
214 made. Additionally, the difference between signal intensity and noise intensity in the UPS2 dataset  
215 is not as great as in other files, and likely the cause of the relatively poor performance across all

216 but XFlow. This relative “flatness” with respect to the other files means that fewer features stand  
217 out, providing XNet with its locality depended thresholding an advantage at picking out low  
218 intensity signals.

219

220 The total number of XICs found in the UPS2 dataset for each algorithm can be seen in Figure 4.

221 **Fig 4. Total Number of XICs Recovered.** The total number of XICs in the set of XICs returned  
222 from each algorithm from the UPS2 dataset. Note the dramatically increased number of XICs by  
223 XFlow compared to existing Algorithms.

224

225

226 The characteristics of a high quality XIC are contiguity along retention time (RT), narrow span  
227 along the m/z axis, and a unimodal distribution of intensity along the RT axis. Exemplary XICs  
228 from each algorithm on the UPS2 data are shown in Figures 5-8.

229

230

231 **Fig 5. XFlow Results.** Selected result of XFlow on the hand annotated data in top-down, 3d and  
232 spectral views. All XICs in window are fully formed, and the extent of the XICs in the RT  
233 dimension are captured. Note that intensity is not unimodal, and likely a result of another envelope  
234 overlapping and adding its intensity to the XICs seen. All algorithms failed to recover these  
235 overlapped XICs.

236 **Fig 6. MzMine2 Results.** Selected result of MzMine on the hand annotated data in top-down 3d  
237 and spectral views. Most XICs in window are fully formed, and XICs extend in the RT dimension  
238 to their full extent. Some of the low intensity XICs have been skipped over, as MzMine2 has  
239 apparently set the intensity threshold too high to accurately capture all the signals. Like XFlow,  
240 MzMine2 has failed to recognize the overlapping signals shown here.

241 **Fig 7. matchedFilter Results** Selected result of matchedFilter on the hand-annotated data in top-  
242 down, 3d and spectral views. One XIC in the center has been completely skipped. Several XICs  
243 extend too far in the m/z dimension. XICs do not extend fully in the RT dimension.

244 **Fig 8: centWave Results.** Result example of centWave in top-down, 3d and spectral views. One  
245 XIC in the center has been completely skipped. Some XICs extend too far in the m/z dimension  
246 as before with matchedFilter. XICs also do not fully extend in RT dimension.

247

248 The number of XICs recovered from alternative datasets for both centroid and profile data can be  
249 observed in Figures 9 and 10.

250 **Fig 9. Total Number of XICs for each Centroid File.** The number of XICs reported by each  
251 algorithm for each centroided dataset. Note the much larger set of XICs returned from XFlow for  
252 the UPS2 data set in comparison to other algorithms, and other files.

253

254 **Fig 10. Total Number of XICs for each Profile File.** The number of XICs reported by each  
255 algorithm for each profile dataset. Note some disparity among mzMine2 and XFlow between  
256 centroid (Figure 9) and profile datasets. *Disparity between profile and centroid, while expected, is*  
257 *not desirable. Ideally, the centroid and profile datasets will have the exact same number of signals*  
258 *as they come from the same source. XCMS's matchedFilter and centWave excelled at recovering*  
259 *the similar numbers of XICs from profile and centroided versions of the datasets.*

260

261

262

263 XCMS' matchedFilter and centWave performed similarly in relation to each other. This is likely  
264 due to the common origin of the algorithms, and IPO's optimization strategy. CentWave and  
265 matchedFilter also had the most similar results between centroid and profile data (Figures 9-10),  
266 also likely attributable to IPOs parameter optimization strategy. The downside of employing IPO  
267 is its very lengthy runtime. Further, while centWave and matchedFilter recovered a greater number  
268 of the hand annotated XICs, they recovered far fewer XICs from the alternative datasets,  
269 qualitatively suggesting that they fail to recover lower intensity signals, an observation that can be  
270 verified by analyzing images from PXD011194 dataset to provide qualitative evaluation and  
271 comparison between algorithms tested. (See Figures 11-14).

272 **Fig 11. Xflow Qualitative Results.** XFlow wide scale (left) and XFlow feature scale (right). It is  
273 clear that XFlow has self-adjusted the intensity slightly too high, and as a result is missing clearly  
274 present XICS (left). Further, XFlow incorrectly splits the leading XIC in the feature view (right)  
275 into two XICs. However, the XICs are well formed, and fully extended, having captured all  
276 relevant points.

277

278 **Fig 12. MzMine2 Qualitative Results.** MzMine2 wide view (left) and feature view (right). The  
279 left view gives the illusion that MzMine2 is selecting for everything not an XIC, however the  
280 feature view (right) shows that MzMine2 is finding the XICs, but fails to capture many of the  
281 points in those XICs.

282

283 **Fig 13. matchedFilter Qualitative Results.** matchedFilter wide view (left) and feature view  
284 (right). The left view shows that matchedFilter manages to return several of the XICs.  
285 MatchedFilter failed to find most of the high intensity points in the feature view (right), but found  
286 several of the peaks.

287

288 **Fig14. centWave Qualitative Results.** centWave wide view (left) and feature view (right). The  
289 left view shows that centWave manages to return several of the XICs. Like matchedFilter,  
290 centWave failed to find most of the points in the XICs in the feature view (right), but found several  
291 peaks.

292 Additionally, it was observed that centWave and matchedFilter both harbor a tendency to over and  
293 under select around regions of interest (Figures 13-14). Additionally, with the prevalence of large  
294 datasets, the runtime of these algorithms is vitally important for their continued feasibility in the  
295 future. These runtimes can be seen below in Figure 15 (note log scale).

296 **Fig 15. Runtime of Algorithms on PXD000792.** This chart shows the log scaled runtimes for  
297 each of the algorithms in seconds on the smallest dataset (PXD000792-Centroid). CentWave took  
298 the longest at ~18000 seconds (approximately 5 hours), matchedFilter and MzMine2 took nearly  
299 the same at about 5 minutes. XFlow took approximately a minute and a half. Note that the time  
300 consuming part of centWave and matchedFilter is the parameter optimization which necessitates  
301 repeated trials to obtain optimal results.

## 302 Discussion

303

304 The results of this study have brought to light several interesting and key features of the ability of  
305 the evaluated algorithms to recover XICs from LC-MS data sets.

306 MZmine2 was the most permissive of the algorithms tested, resulting in the most XICs recovered  
307 compared to the other algorithms (except for XFlow and UPS2) but failed to recover many XICs  
308 for the UPS2 dataset, recovering only 18%. Additionally, MZmine2 suffered some disparity  
309 between centroided and profile datasets, particularly on PXD000792, a particularly small and low-  
310 resolution file. MZmine2 can be qualitatively observed to be too permissive, as many noise points

311 are included as signals (Figure 12), additionally, signal points are often excluded from  
312 classification.

313 Considering the total number of XICs collected for each algorithm with respect to each data file,  
314 it is clear here that the UPS2 dataset has interesting qualities in relation to the other datasets (Figure  
315 4). XFlow returned the most hand annotated XICs between any algorithm, and MzMine2 returned  
316 far fewer XICs from the UPS2 dataset than any other file, this disparity seems only attributable to  
317 something inherent in the dataset itself, likely as mentioned before, the relatively small difference  
318 between the signal intensity, and the background noise intensity in the dataset.

319 The runtime of the algorithms is highly disparate, and the challenges of optimizing a highly  
320 parameterized algorithm such as centWave (Even using an automated tool like IPO) is  
321 prohibitively time consuming for larger datasets. It is feasible to reuse optimized parameters, but  
322 doing so is likely to return suboptimal results. In this way, it is clear that parameterless approaches  
323 will excel.

## 324 Conclusion

325 The size of the datasets, the complexity of the signals, and the noise obfuscation make XIC  
326 acquisition from MS1 data extremely challenging. The general method to account for complexity  
327 has been to include parameters to increase the scope of an individual algorithm. It was our goal in  
328 our lab to reduce complexity, and simplify the experience of conducting MS1 analysis by  
329 designing XFlow in a procedurally agnostic way such that it works on a wide variety of MS1  
330 datasets without parameter modification regardless of centroiding or instrument type, a goal that  
331 is now accomplished. It's clear that XFlow excels at signal acquisition for the UPS2 dataset in  
332 particular and performs favorably with respect to other algorithms in signal acquisition from  
333 alternate datasets (Figures 11-14). Additionally, while qualitative information is gained by

334 comparing results for alternative datasets, it's impossible to quantitatively evaluate the  
335 performance of the algorithms for datasets that do not have a hand annotated version. To this end,  
336 developing a database of a variety of hand annotated datasets with which to evaluate algorithms  
337 remains a valuable endeavor, in order to provide additional sources of comparison beyond UPS2.  
338

339 Author contributions

340 M.G. wrote XFlow, ran evaluation experiments, curated and interpreted results. R.S. conceived  
341 the algorithm and designed and supervised the project. All authors contributed to the manuscript.

342 Conflict of interest

343 Authors declare no conflict of interest.

344 Availability

345 XFlow is available at [github.com/optimusmoose/XFlow](https://github.com/optimusmoose/XFlow) with an Apache 2.0 license. Funding

346 Funding

347 This research was supported by NSF grant number 366208 to R.S.

348

349 Materials & correspondence

350 Should be directed to R.S.

351

## 352 References

- 353 1) Smith R. Conversations with 100 Scientists in the Field Reveal a Bifurcated Perception of  
354 the State of Mass Spectrometry Software. *Journal of Proteome Research* 2018 17 (4),  
355 1335-1339 DOI: 10.1021/acs.jproteome.8b00015
- 356 2) Smith R, Ventura D, Prince J. LC-MS alignment in theory and practice: a comprehensive  
357 algorithmic review, *Briefings in Bioinformatics* 16(1), 2015, Pages 104–117, DOI:  
358 10.1093/bib/bbt080
- 359
- 360 3) Smith R, Ventura D, Prince J. Novel algorithms and the benefits of comparative validation,  
361 *Bioinformatic* 29(12), 2013, Pages 1583–1585, DOI: 10.1093/bioinformatics/btt176
- 362
- 363 4) Bertsch A, Gropf C, Reinert K, Kohlbacher O. OpenMS and TOPP: Open Source Software  
364 for LC-mS Data Analysis. *Data mining in Proteomics: From Standards to Applications*;  
365 Humana Press, 2011; Pages 353-367.
- 366
- 367
- 368 5) Smith R, Taylor R.M, Prince J.T. Current controlled vocabularies are insufficient to  
369 uniquely map molecular entities to mass spectrometry signal. *BMC Bioinformatics* 16(S2)  
370 2015. DOI:10.1186/1471-2105-16-S7-S2
- 371
- 372 6) Gutierrez M, Handy K, and Smith R. XNet: A Bayesian Approach to Extracted Ion  
373 Chromatogram Clustering for Precursor Mass Spectrometry Data. *Journal of Proteome*  
374 *Research* 18(7), 2019, Pages 2771-2778. DOI: 10.1021/acs.jproteome.9b00068
- 375
- 376 7) Tostengard A, and Smith R. “A Quantitative Evaluation of Ion Chromatogram Extraction  
377 Algorithms” *Journal of Proteome Research* (in review).
- 378
- 379 8) Conley C, Smith R, Torgrip R, Taylor R, Tautenhahn R, Prince J. Massifquant: open-  
380 source Kalman filter-based XC-MS isotope trace feature detection, *Bioinformatics* 30(18),  
381 2014. Pages 2636–2643, DOI: 10.1093/bioinformatics/btu359
- 382
- 383 9) Smith C, Want E, O'Maille G, Abagyan R, Siuzdak G. Processing Mass Spectrometry  
384 Data for Metabolite Profiling Using Nonlinear Peak Alignment, Matching, and  
385 Identification. *Analytical Chemistry* 78 (3), 2006. Pages 779-787. DOI:  
386 10.1021/ac051437y
- 387
- 388 10) Tautenhahn R, Böttcher C, Neumann, S. Highly sensitive feature detection for high  
389 resolution LC/MS. *BMC Bioinformatics* 9(504), 2008. DOI:10.1186/1471-2105-9-504
- 390
- 391 11) Cox J, Mann M. MaxQuant enables high peptide identification rates, individualized p.p.b.-  
392 range mass accuracies and proteome-wide protein quantification. *Nat Biotechnol* 26, Pages  
393 1367–1372 (2008) DOI:10.1038/nbt.1511

394

395

396 12) Zhurov K, Kozhinov A, Fornelli L, Tsybin Y. Distinguishing Analyte from Noise  
397 Components in Mass Spectra of Complex Samples: Where to Cut the Noise? *Analytical*  
398 *Chemistry* 86(7), 2014. 3308-3316 DOI: 10.1021/ac403278t

399

400

401 13) Sedgewick R. *Algorithms in Java*, Parts 1–4: Fundamentals, Data Structures, Sorting,  
402 and Searching, Addison–Wesley.

403

404

405 14) Henning J, Tostengard A, Smith R. A Peptide-Level Fully Annotated Data Set for  
406 Quantitative Evaluation of Precursor-Aware Mass Spectrometry Data Processing  
407 Algorithms *Journal of Proteome Research* 18(1), 2019. Pages 392-398. DOI:  
10.1021/acs.jproteome.8b00659

408

409 15) Chih-Chiang T, Avtonomov D, Larsen B, Tucholska M, Choi H, Gingras A, Nesvizhskii  
410 A. DIA-Umpire: comprehensive computational framework for data-independent  
411 acquisition proteomics. *Nature Methods* 12(3), 2015.

412

413 16) Pluskal T, Castillo S, Villar-Briones A, Orešić M. MZmine 2: Modular framework for  
414 processing, visualizing, and analyzing mass spectrometry-based molecular profile data.  
415 *BMC Bioinformatics* 11(395), 2010. DOI:10.1186/1471-2105-11-395

416

417 17) Libiseller G, Dvorzak M, Kleb U, Gander E, Eisenberg T, Madeo F et al. IPO: a tool for  
418 automated optimization of XCMS parameters. *BMC Bioinformatics* 16(118), 2015.  
419 DOI:10.1186/s12859-015-0562-8

420

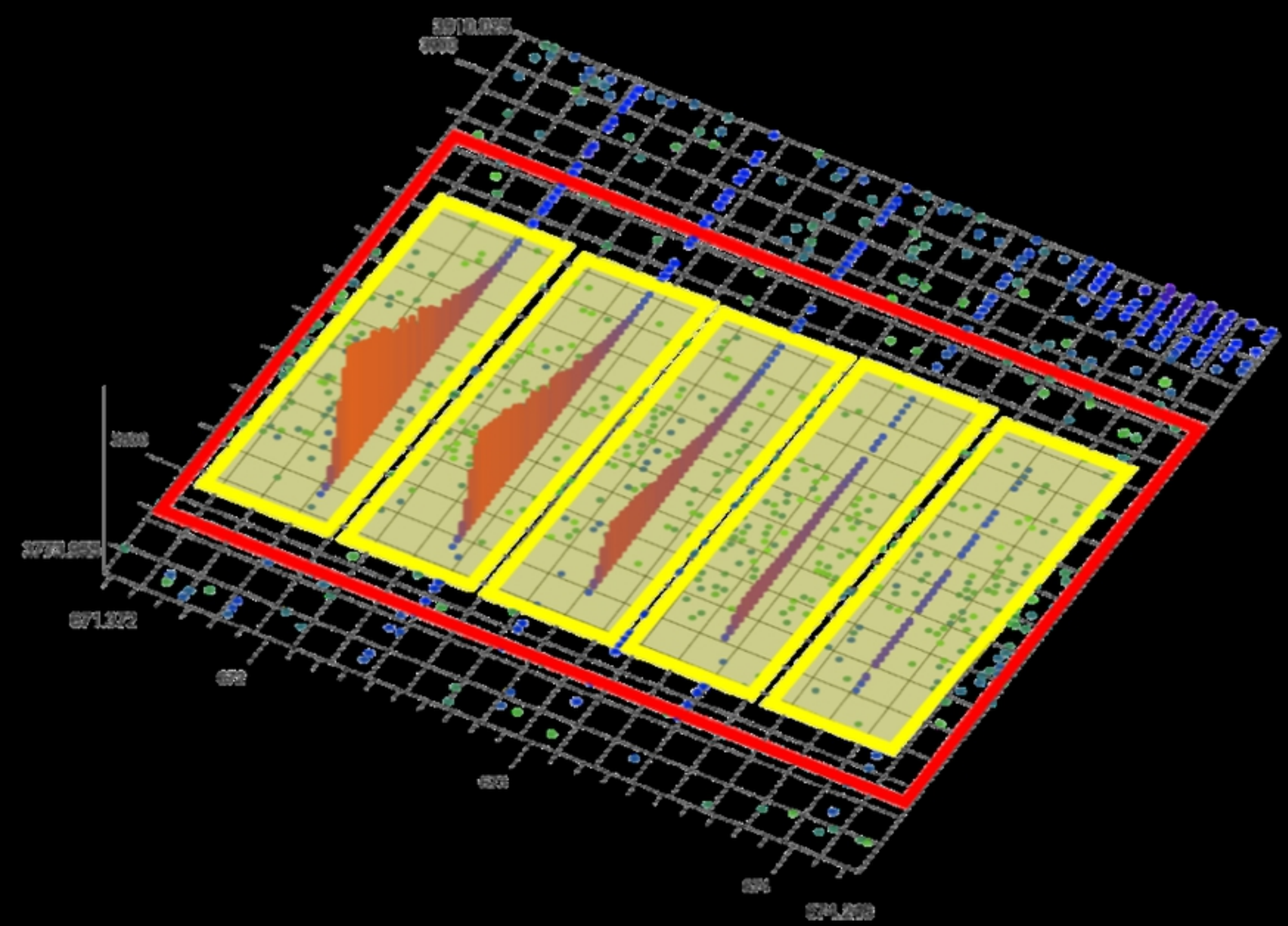
421 18) Kessner D, Chambers M, Burke R, Agus D, Mallick P, ProteoWizard: open source  
422 software for rapid proteomics tools development, *Bioinformatics* 24(21), 2008. Pages  
423 2534–2536, DOI: 10.1093/bioinformatics/btn323

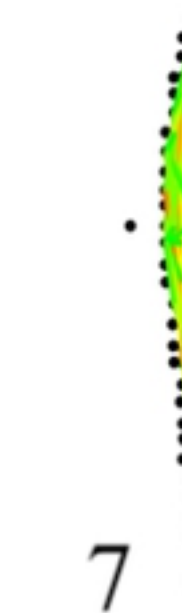
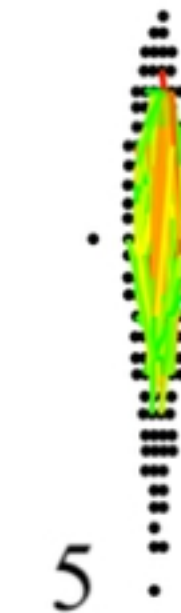
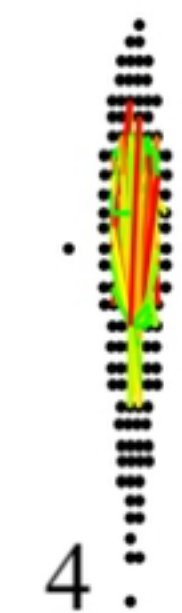
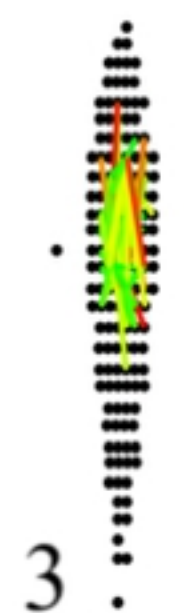
424

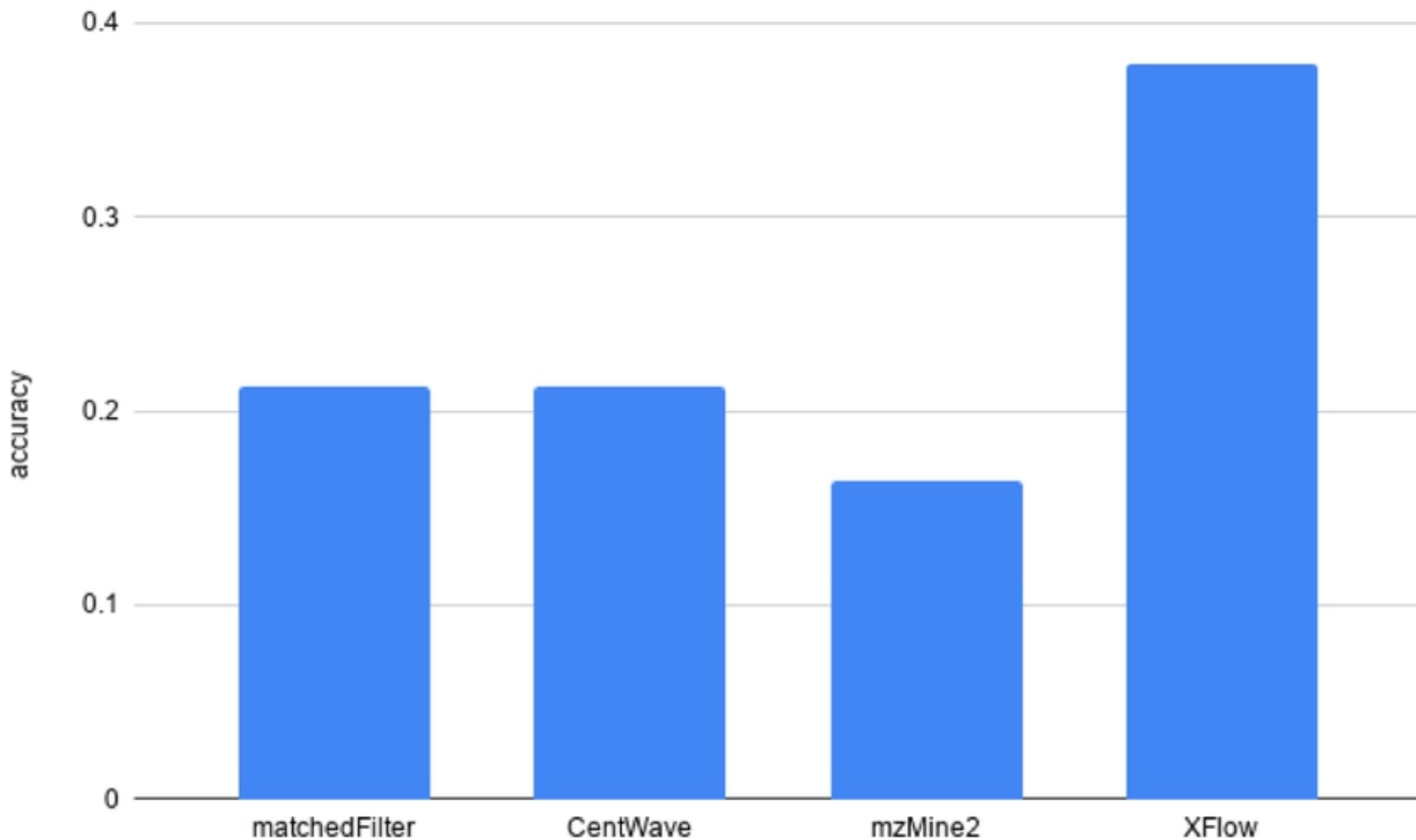
425 

## Supporting Information

426 XFlow and additional information is available at [github.com/optimusmoose/jsms](https://github.com/optimusmoose/jsms) with an MIT  
427 license







Number of XICs recovered

125000

100000

75000

50000

25000

0

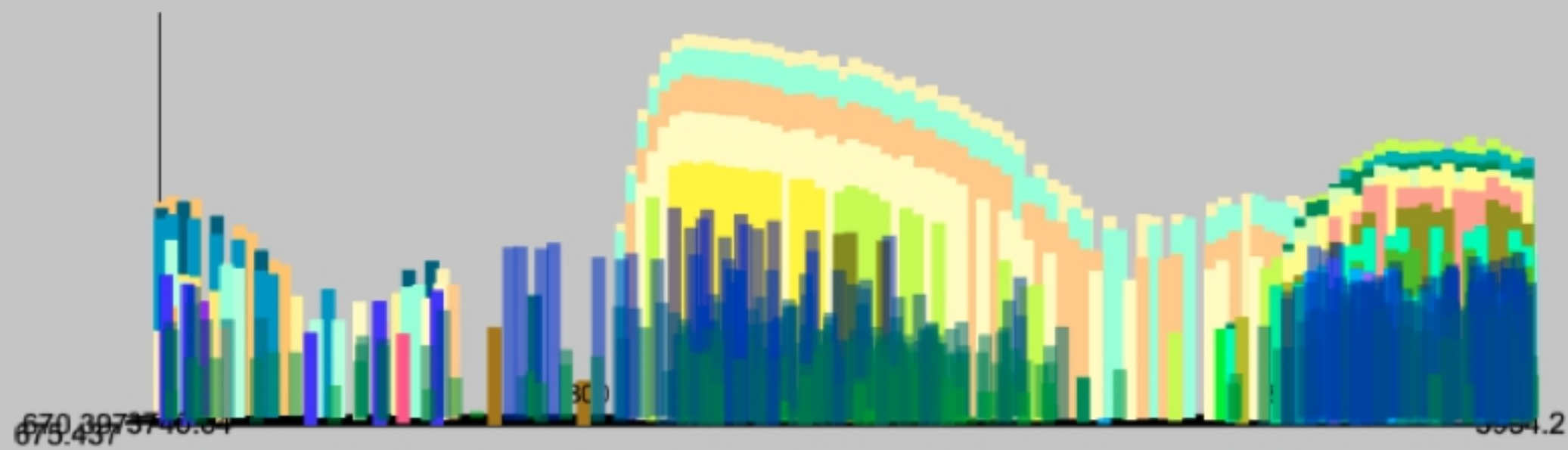
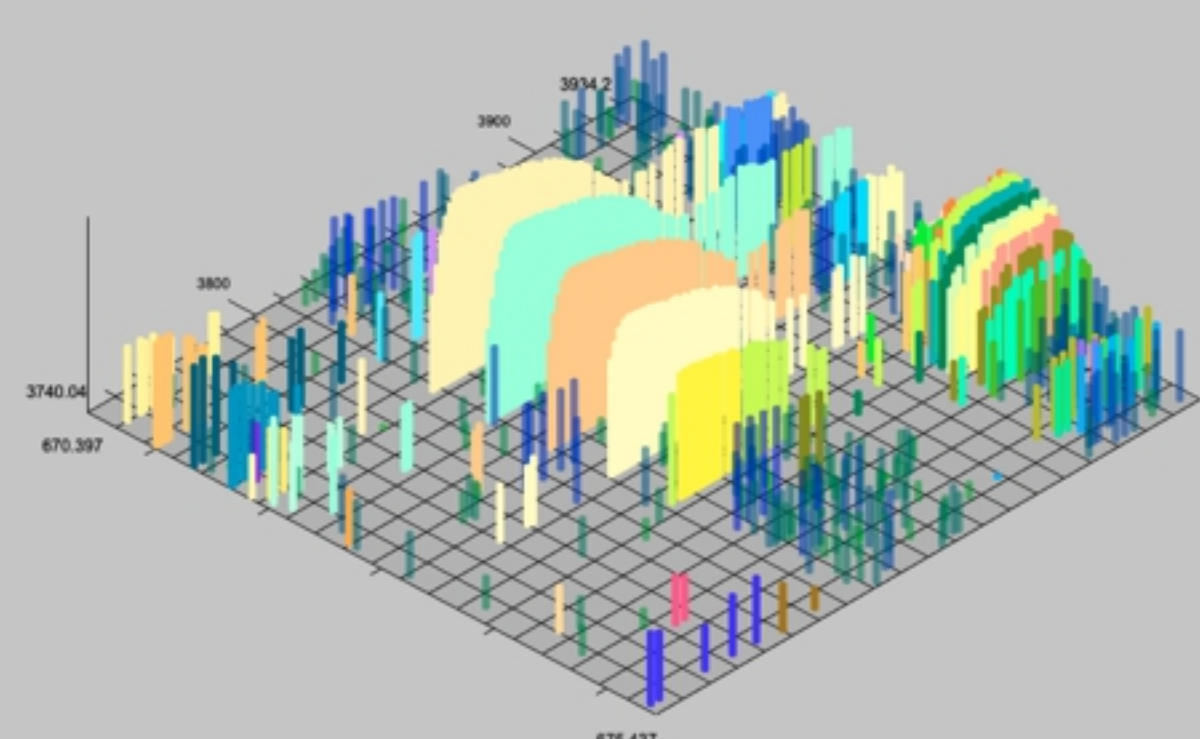
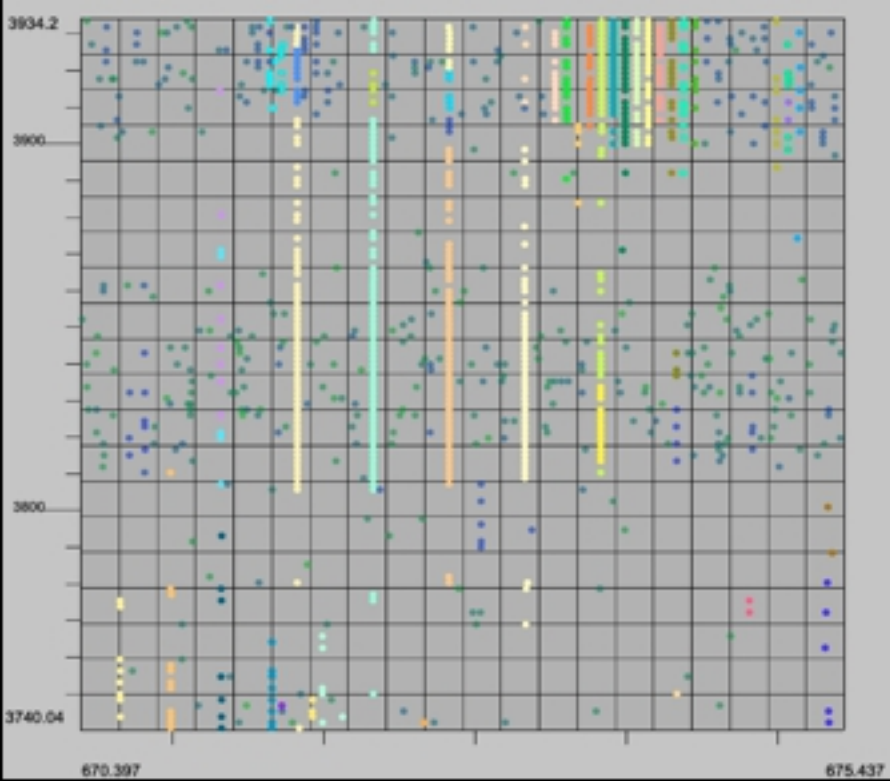
matchedFilter

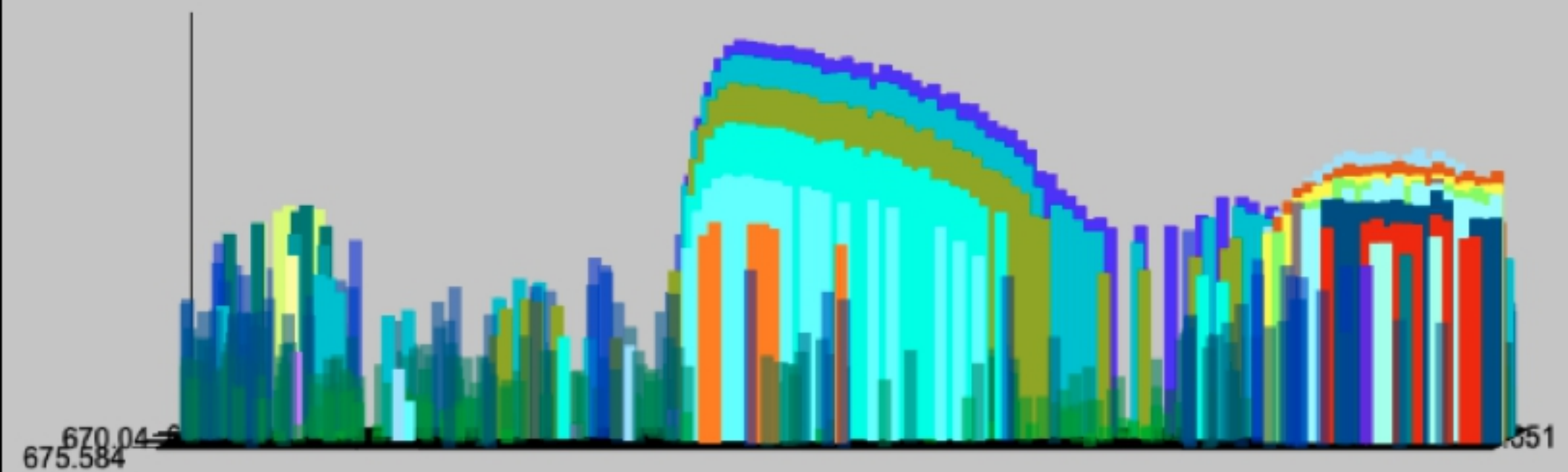
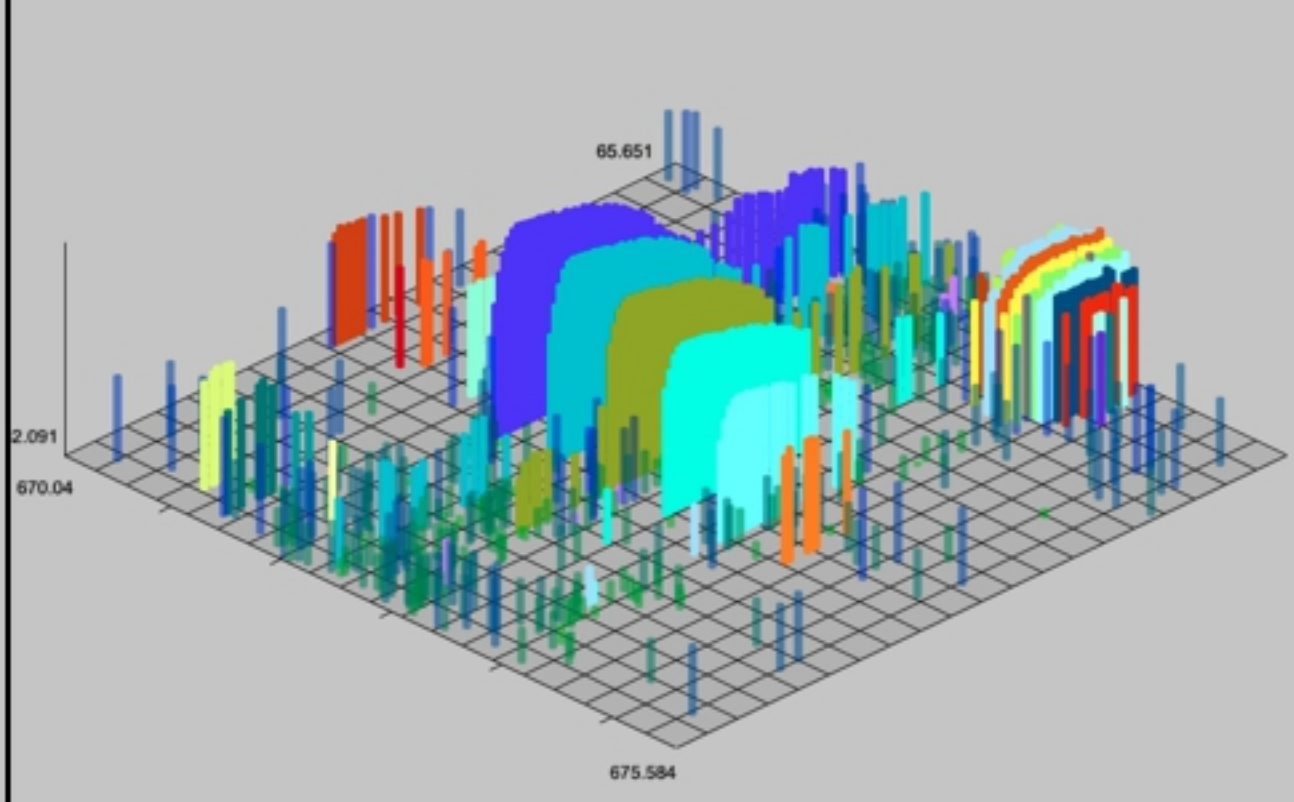
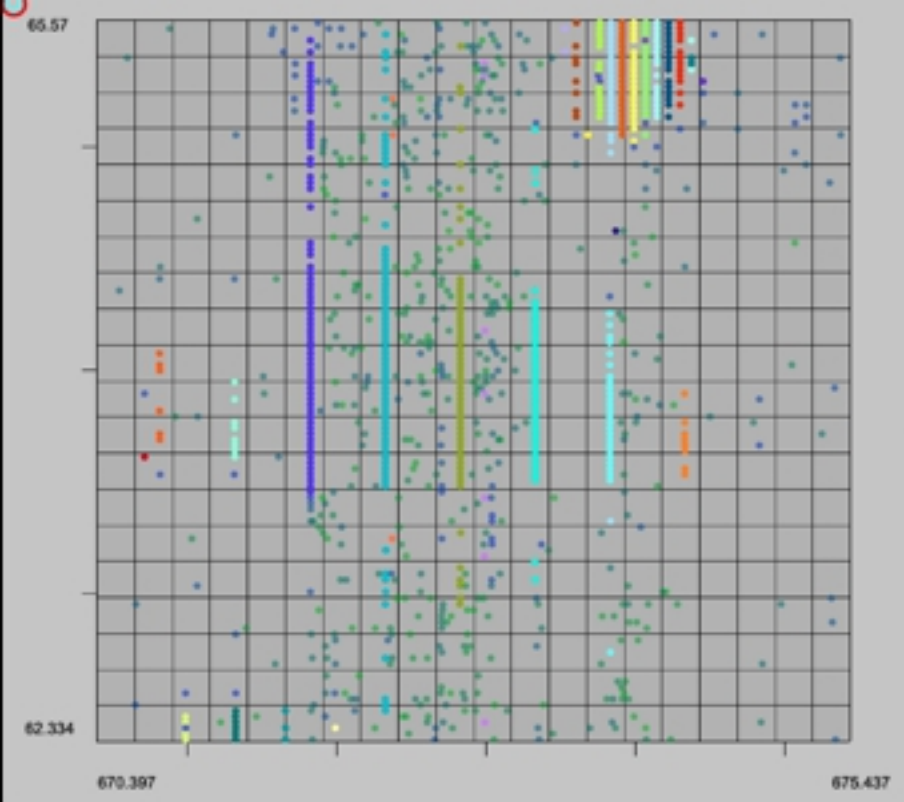
CentWave

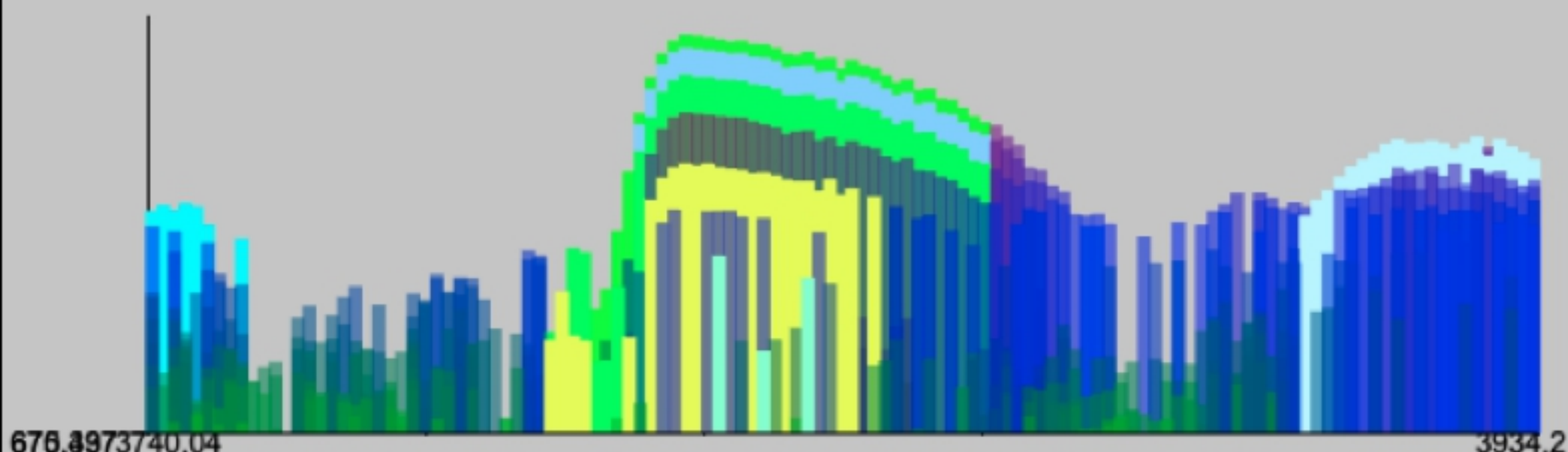
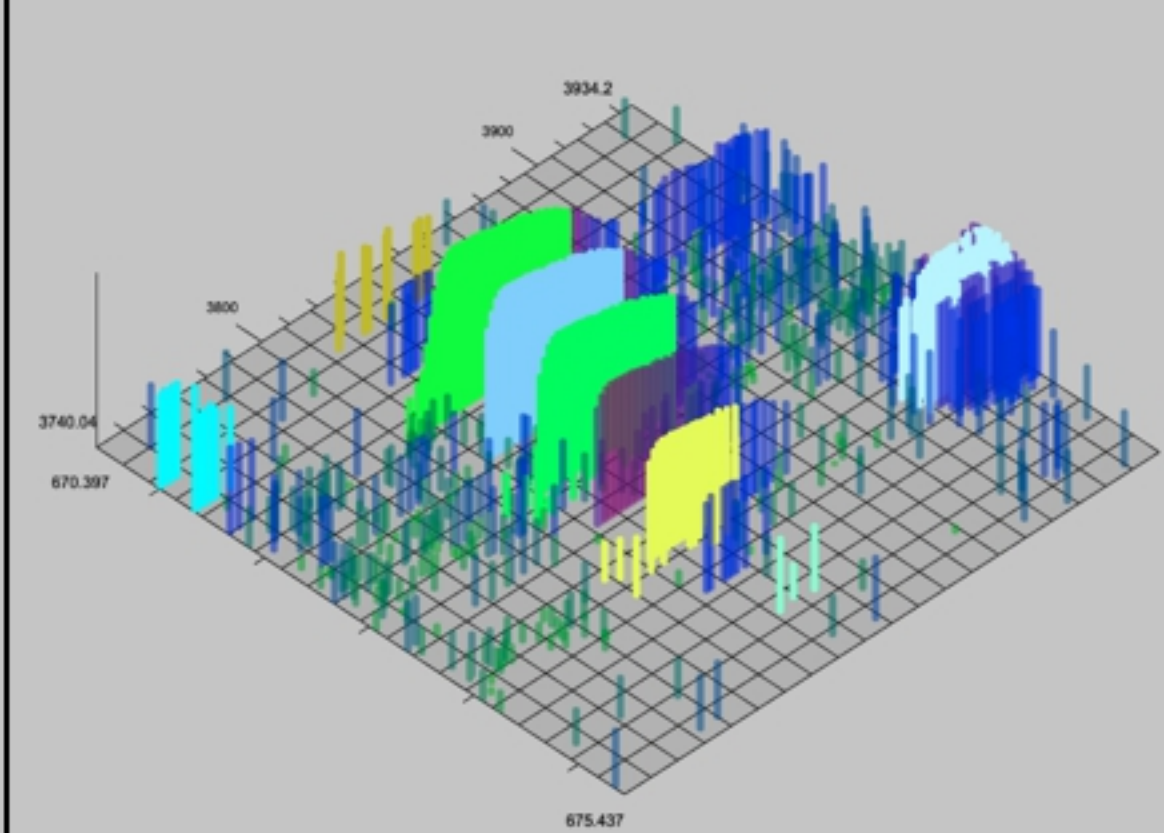
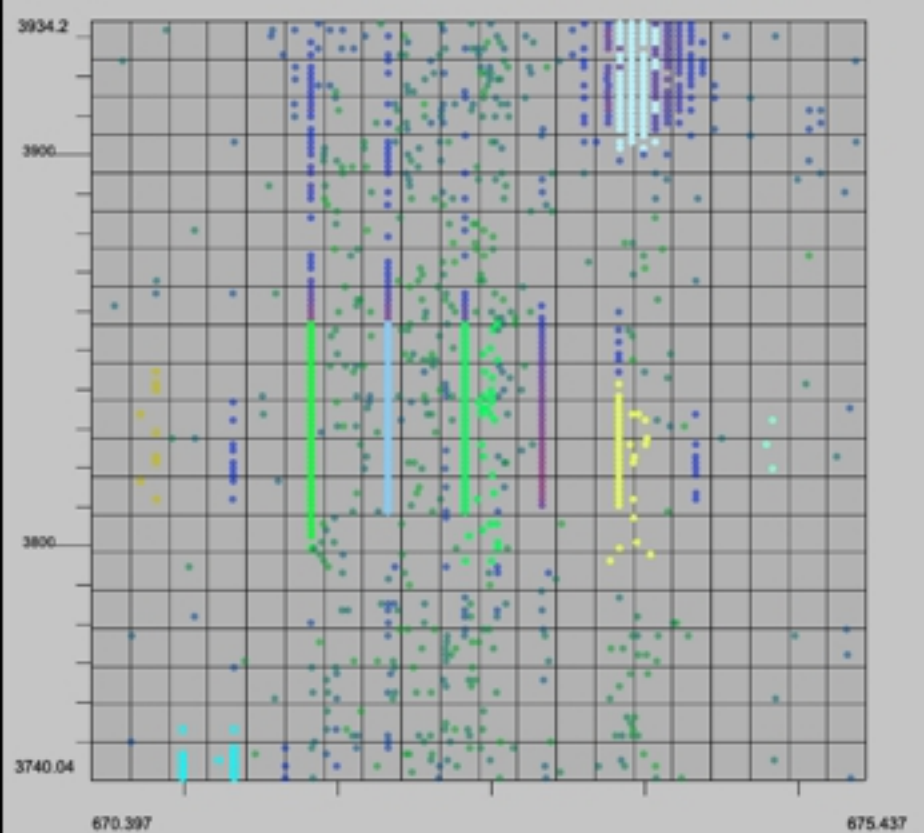
mzMine2

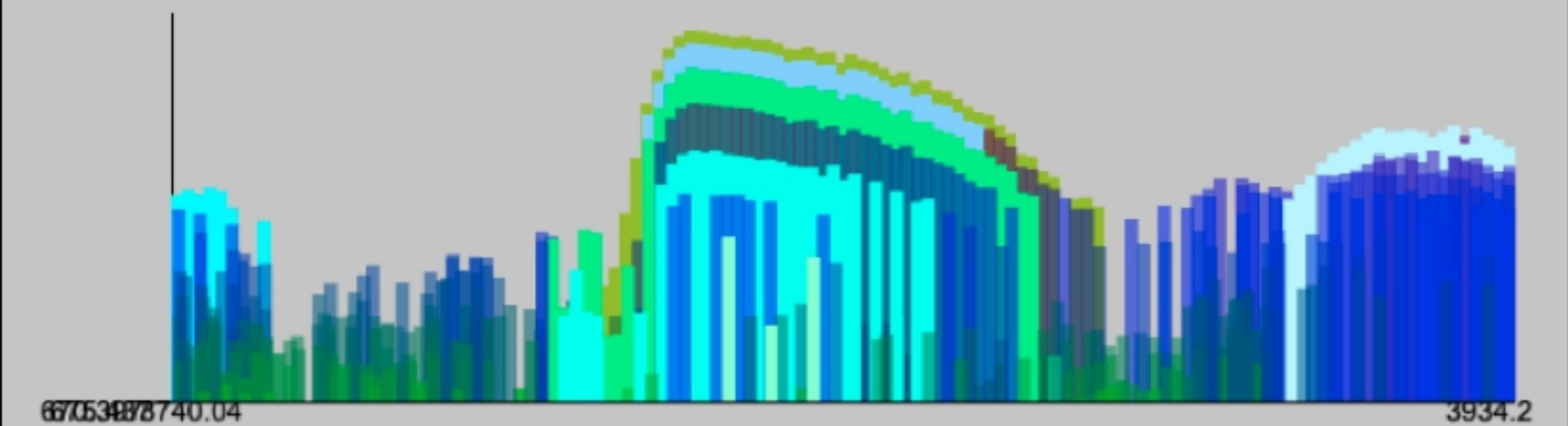
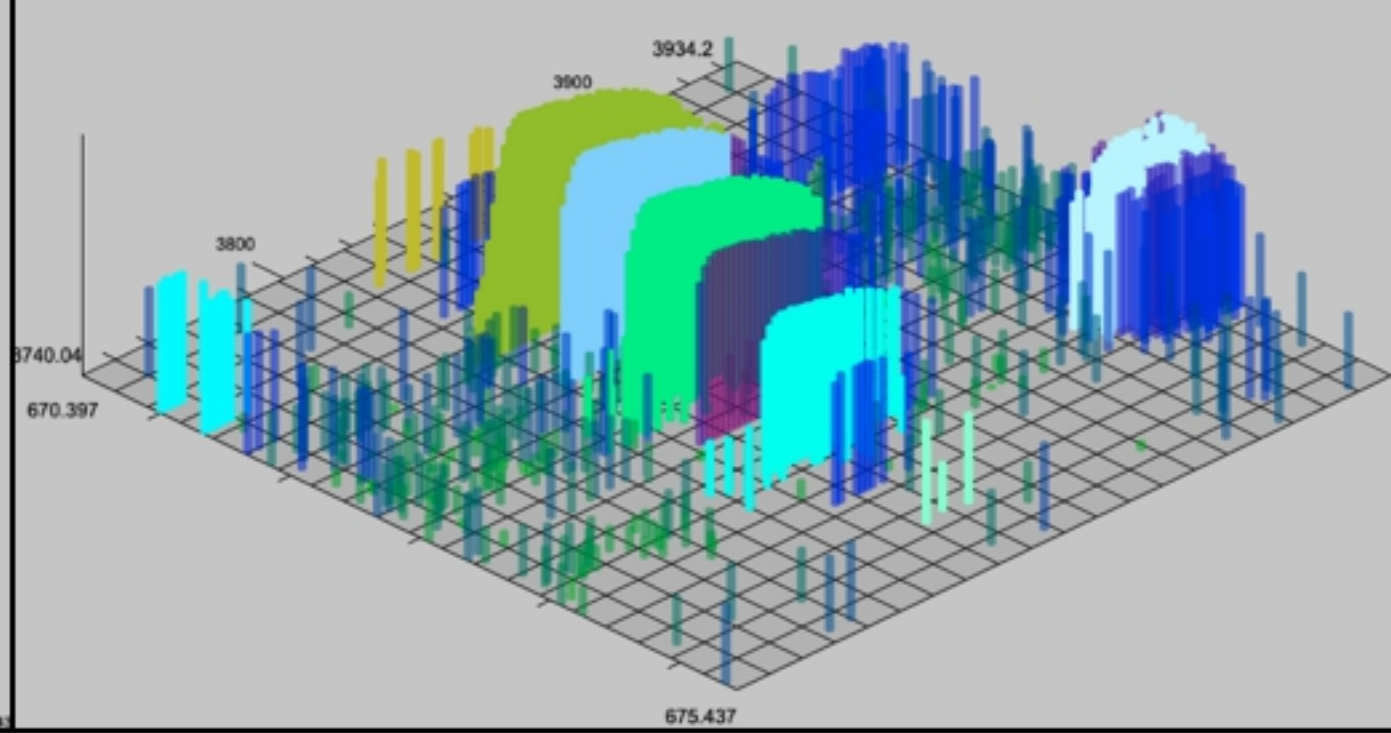
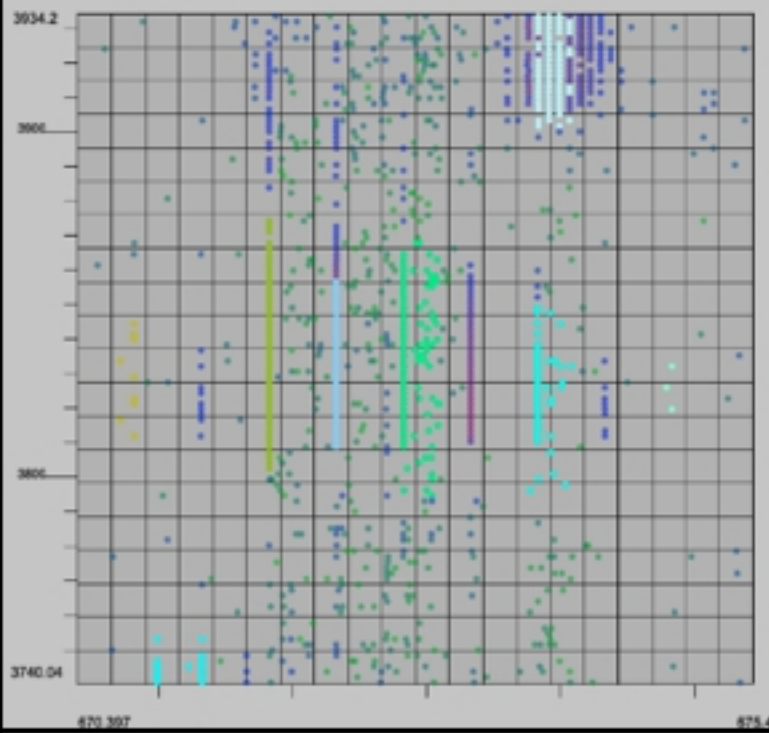
XFlow

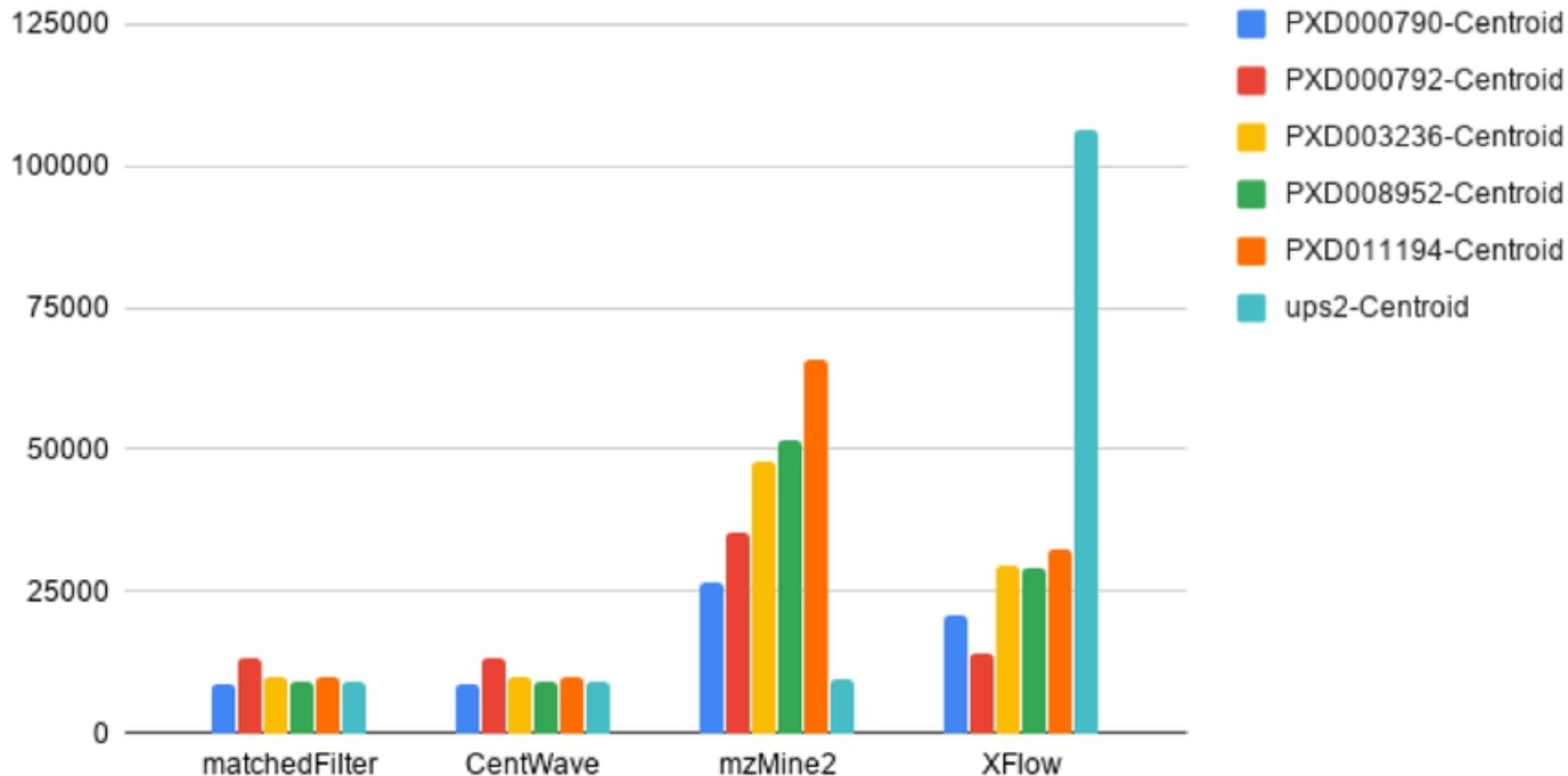


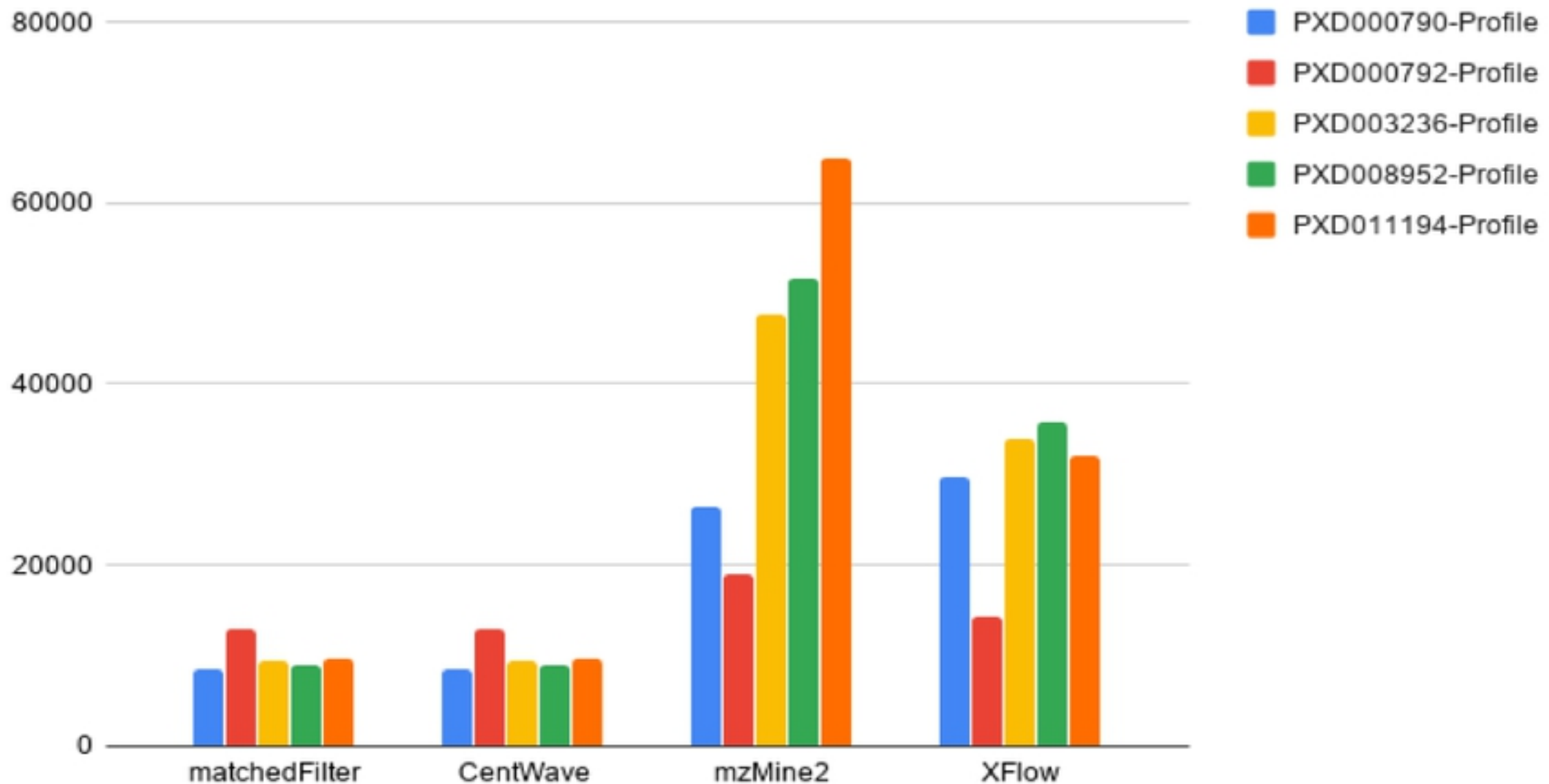


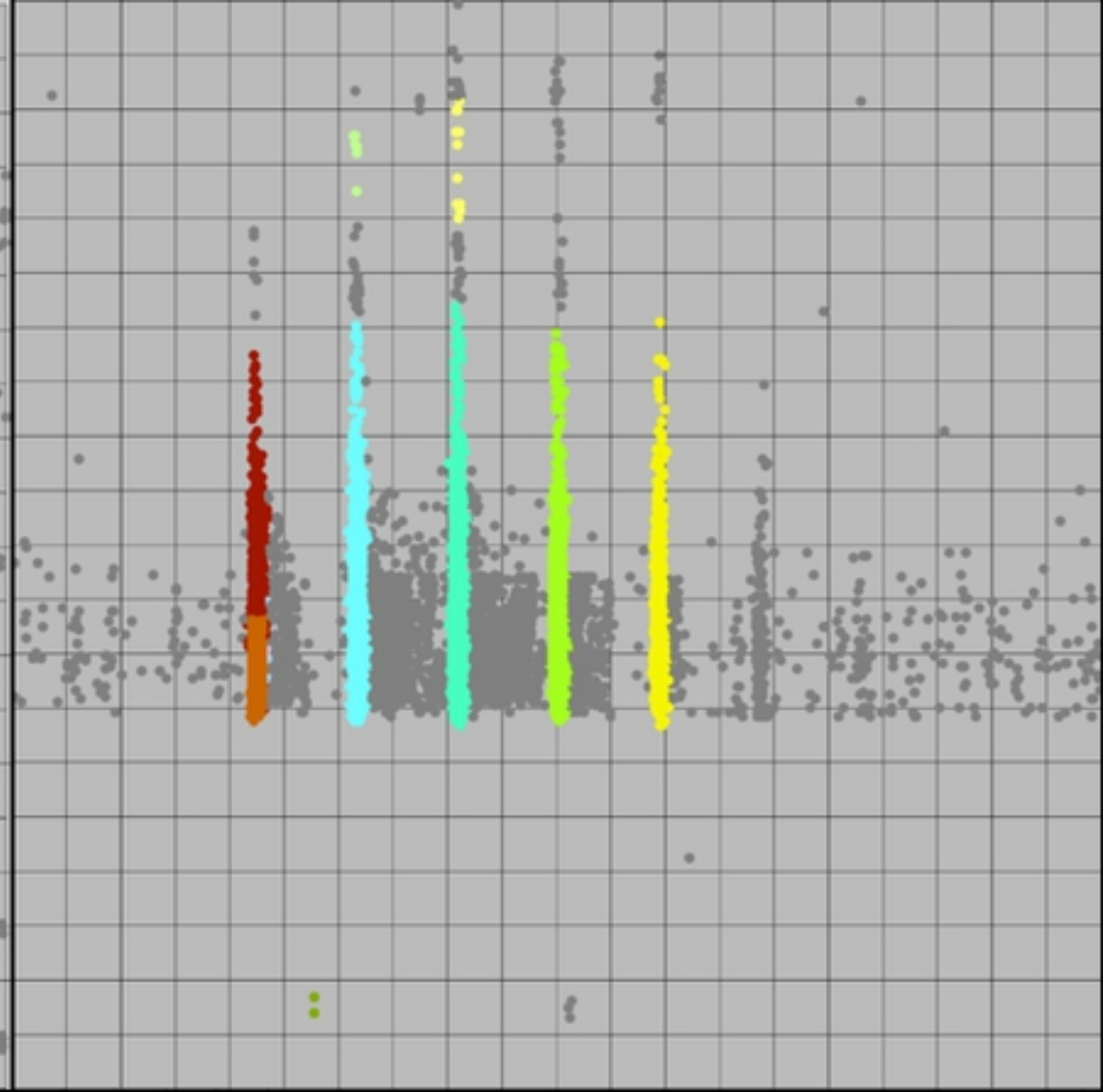
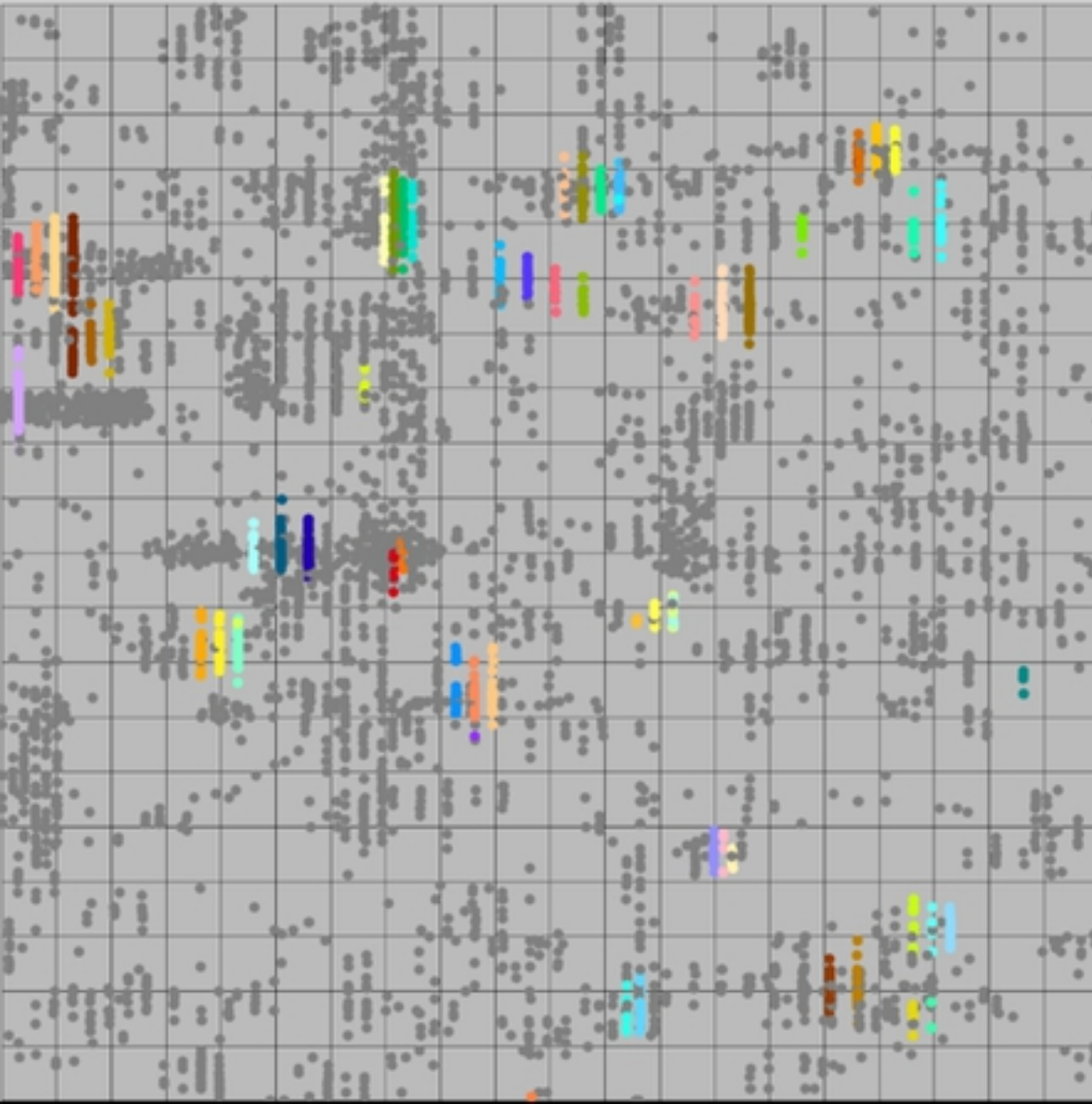


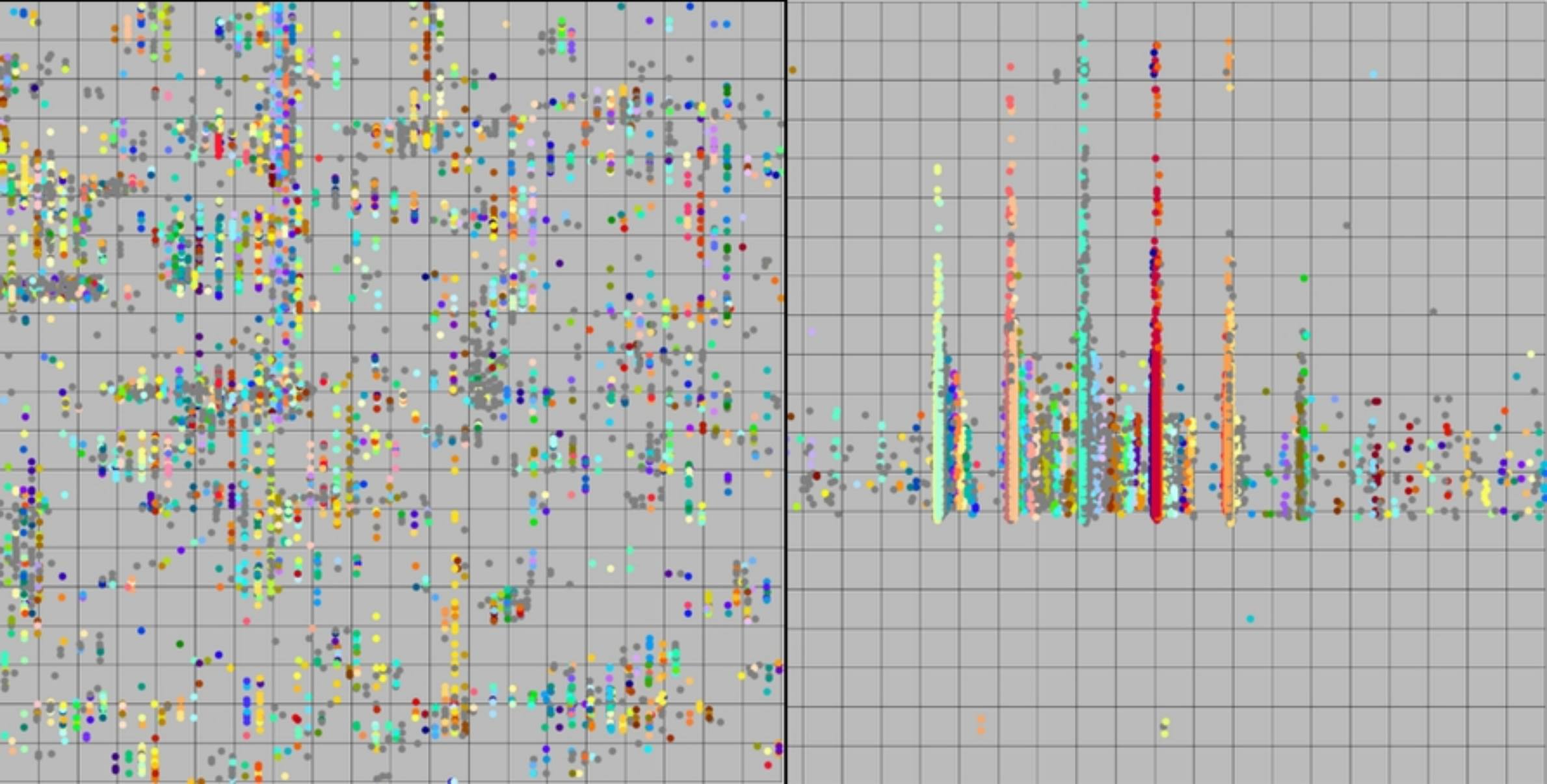


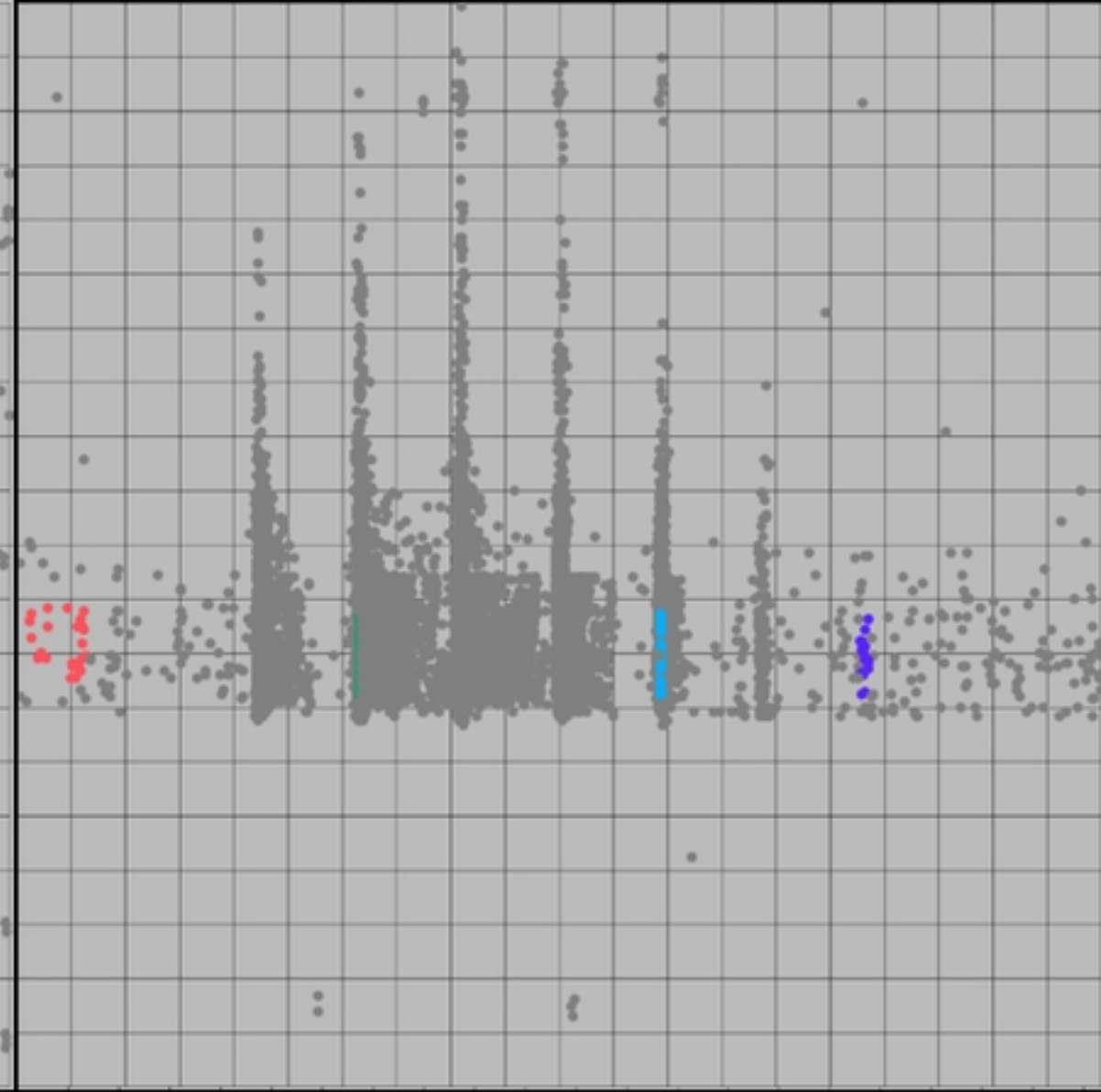
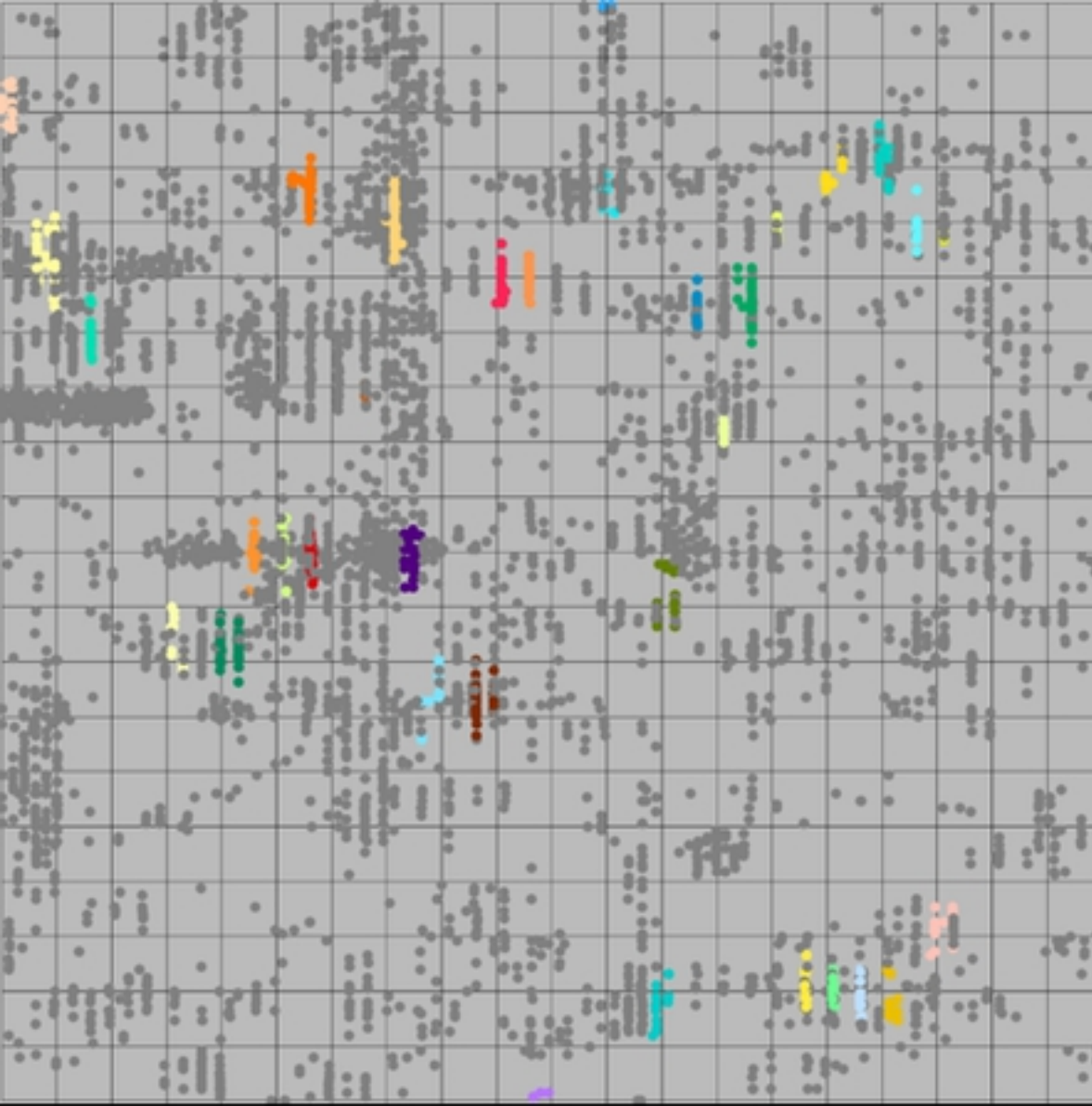


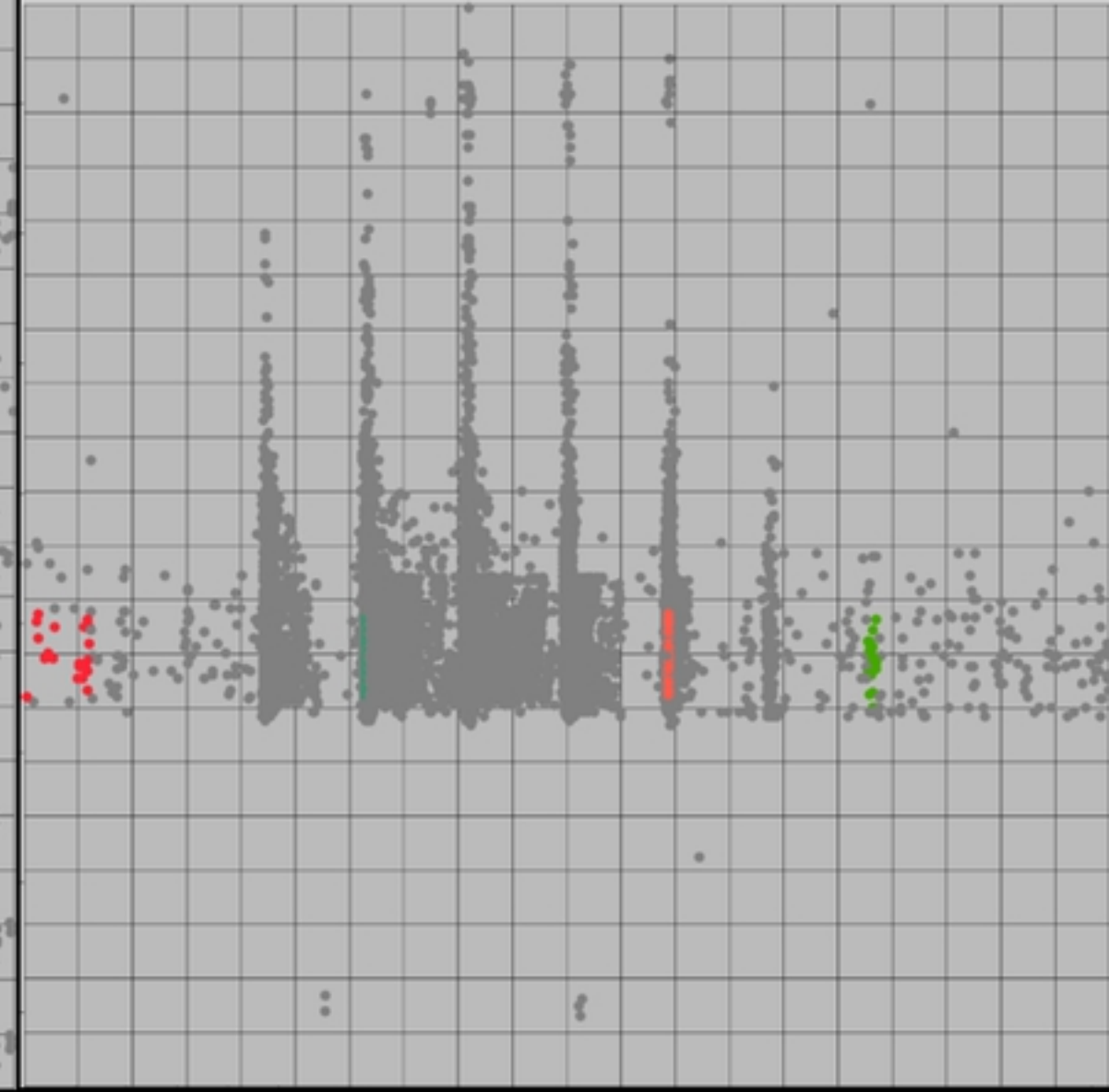
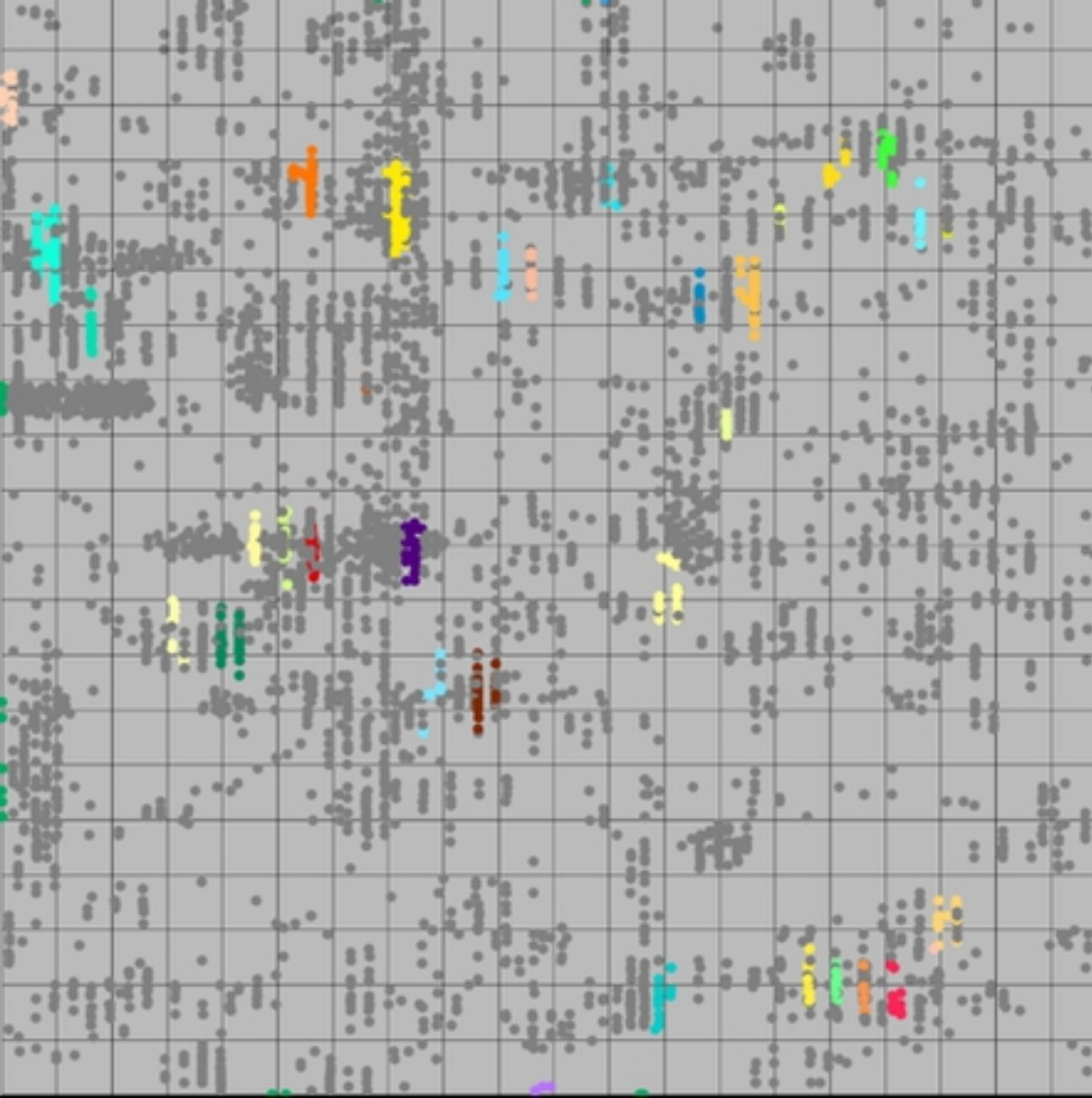












# Runtime

